STUDIA UNIVERSITATIS BABEŞ-BOLYAI BIOLOGIA, 71, 1, 2026 (p. 39-57)
doi:10.24193/subbbiol.2026.1.03

Doxorubicin toxicity: Histological and ultrastructural tissue damage

Emilia Anca[1], Corina Roşioru[2], Vlad-Alexandru Toma[2,3], Lucian Barbu-Tudoran[2,3,4,5], Septimiu Tripon[4,5], Anca-Daniela Stoica[2,3], and Camelia Dobre[2,3]✉

[1]Doctoral School of Integrative Biology, Faculty of Biology and Geology, Babeş-Bolyai University, Cluj-Napoca, Romania; [2]Faculty of Biology and Geology and Center of Systems Biology, Biodiversity and Bioresources, Babeş-Bolyai University, Cluj-Napoca, Romania; [3]Department of Molecular Biology and Biotechnology, Babeş-Bolyai University, Cluj-Napoca, Romania; [4]Electron Microscopy Laboratory "Prof. C. Crăciun", Faculty of Biology and Geology, Babeş-Bolyai University, Cluj-Napoca, Romania; [5]Electron Microscopy Integrated Laboratory, National Institute for Research and Development of Isotopic and Molecular Technologies, Cluj-Napoca, Romania
✉***Corresponding author, E-mail: camelia.lang@ubbcluj.ro***

Article history: Received 3 April 2025; Revised 1 April 2026; Accepted 2 June 2026; Available online 25 June 2026

Abstract. Doxorubicin (DOX) is an effective chemotherapeutic with known toxic effects over the liver, kidneys and most importantly the heart. DOX effects, such as oxidative stress induction, topoisomerase II poisoning and activation of pro-inflammatory pathways are a double-edged sword. While enhancing the antitumoral activity of this agent, these mechanisms also contribute to tissue damage which limits its use. To build upon previous research that evaluated circulating biomarkers of DOX-induced cardiac toxicity, this study offers additional perspectives on structural effects on tissues along with a short literature review of DOX use.

Keywords: doxorubicin, pharmacological toxicity, histopathology, ultrastructural analysis

Introduction

Anthracyclines are a class of drugs firstly classified as antibiotics at the moment of their discovery in 1939, when daunorubicin was isolated from *Streptomyces peucetius*. Their antitumoral effects were only found over a decade later and represented a groundbreaking achievement for the field of Oncology. This event led to the discovery of several other anthracyclines such as idarubicin, epirubicin and most importantly, doxorubicin (DOX) (Shandilya *et al*., 2020; Xie *et al*., 2024).

General information and uses. DOX, also known as Adriamycin, was first extracted from *Streptomyces peucetius var. caesius* and has been an important drug in the fight against cancer ever since its entry in clinical trials in 1969 (Cassinelli, 2016). It received Food and Drug Administration (FDA) approval in 1974 (Jones and Dass, 2022) and it is included in the World Health Organization (WHO) List of Essential Medicines (WHO, 2023). DOX is used in the treatment of a wide range of cancers, including solid tumors of the breast, bladder, soft tissue and tumors of the hematopoietic and lymphoid tissues, in both pediatric and adult patients (Rawat *et al*., 2021). It is used in veterinary medicine as a cancer treatment as well (Liu *et al*., 2024).

While many DOX formulations have been developed to improve drug efficiency such as liposomes and polymeric-based platforms, few reached the clinical trial stage (Lee *et al*., 2023). In current clinical practice, DOX is used as a hydrochloride salt ("free form") or a liposomal formulation (Li *et al*., 2022).

Liposomal DOX, branded as DoxilÒ, LipodoxÒ or CaelyxÒ, is a nanoformulation consisting of a conjugation of the drug with polyethylene glycol (PEG) which offers a longer circulation time, higher uptake in tumor sites and an enhanced stability of DOX. A non-PEGylated DOX, MyocetÒ is a liposomal formulation containing phosphatidylcholine and cholesterol which also increases its circulation time (Leung *et al*., 2019; van den Boogaard *et al*., 2022).

Other nanoformulations, based on hydrogels, alginate particles and nano-emulsions are constantly being developed and tested. Promising results were obtained by encapsulating DOX in "ferritin cages", which besides the advantages of liposomal formulations, are able to target cancer cells more efficiently (Lee *et al*., 2023; Mattioli *et al*., 2023).

Mechanism of action. The antitumoral effect of DOX is exerted through multiple mechanisms, most of which are not well understood yet. The most potent mechanisms involve DNA damage through intercalation and topoisomerase 2 (TOP2) poisoning, and the overproduction of reactive oxygen species (ROS) which increase oxidative stress and trigger cell death. Additionally, DOX has other less impactful mechanisms that contribute to this effect: senescence and cell

death by iron and calcium homeostasis disruption, and alteration of biological membranes.

Topoisomerase II poisoning and DNA intercalation. TOP2 is an essential enzyme capable of reducing torsional stress created during transcription and replication. These processes create supercoils and tangles in the DNA, and TOP2 fixes them by creating temporary double-strand breaks to allow uncoiling (Yang *et al*., 2014).

DOX intercalates into DNA and blocks the activity of TOP2 right after the double break step and prevents ligation, which activates the DNA damage response. Once activated, the cell cycle is arrested and cell death signaling pathways are initiated. This mechanism is also responsible for some of its side effects (Kciuk *et al*., 2023; van der Zanden *et al*., 2021).

TOP2a is the major isoform of the enzyme and the main target of DOX because of its prevalence in fast-dividing cells, whereas the b isoform is more present in non-dividing or terminally differentiated cells, such as cardiomyocytes where this mechanism contributes to CTOX (Yang *et al*., 2014).

DOX-DNA adducts formation and chromatin damage. This mechanism has a strong relationship to TOP2 poisoning but is treated in literature as a separate mechanism. The binding of DOX into the DNA helix activates damage responses itself and is facilitated by formaldehyde that comes from the interaction between free radicals and lipids. Although adduct formation does not have a meaningful impact on cancer cells, the addition of formaldehyde-forming compounds to the chemotherapeutic regimen was proven beneficial (Yang *et al*., 2014).

Another effect of DOX-DNA complexes is chromatin damage through histone eviction which leads to mostly epigenomic changes, but the transcriptional landscape modifications are notable as well. An example of this mechanism consists in the expression of oxidative stress- and cell death-related genes (Jones and Dass, 2022; van der Zanden *et al*., 2021).

ROS-induced damage. Oxidative stress represents an imbalance between ROS production and the activity of the antioxidant defense system - comprised of enzymes and antioxidants (Shi *et al*., 2023).

ROS are fundamental for cell signaling processes and immune system function, if present at physiological levels and given that the cell's antioxidant system function properly (Forman *et al*., 2010). DOX metabolization leads to the overproduction of ROS, effect that can be imagined as a double-edged sword. While ROS and increased oxidative stress are crucial in the antitumoral effect of DOX, these also lead to cellular injury in healthy tissues and notorious side effects that limit its use.

DOX has a high affinity for cardiolipin, a lipid found in the inner mitochondrial membrane. The interaction between these molecules inhibits the activity of the

electron transport chain (ETC) and accumulates DOX in this cell compartment. Oxidoreductases found here produce superoxide radicals from the quinone moiety of DOX, which are converted by superoxide dismutase (SOD) into hydrogen peroxide (H_2O_2), to reduce its damaging power. In the presence of Fe^{2+} (which accumulates in the mitochondria due to DOX), H_2O_2 is converted into the more potent hydroxyl radical. Because this cannot be detoxified by the enzymatic antioxidants, its presence leads to nucleic acid damage and lipid peroxidation (Shi *et al*., 2023). The peroxidation of lipid membranes increases the concentration of aldehydic compounds, which in turn produce more ROS and activates cell death pathways (Christidi and Brunham, 2021).

DOX-induced cell death. Autophagy is a response triggered by cell stress and consists of cell degradation followed by the recycling of useful components in the process. In DOX treatment, this is stimulated by mitochondrial damage and oxidative stress and is considered an antitumoral mechanism if cellular DOX concentration is under a toxic threshold. High or chronic exposure is associated with suppression of this process which is known to promote tumor development and drug resistance (Kciuk *et al*., 2023).

Necroptosis, another form of cell death is mediated by tumor necrosis factor alpha (TNFa) signaling, which activates the formation of the necroptosome complex. This leads to cell membrane rupture and the release of cellular components that trigger immune responses (Christidi and Brunham, 2021).

Ferroptosis is an iron-dependent form of cell death that is strictly tied to ROS accumulation. DOX, and its main metabolite, doxorubicinol stop iron metabolism by making iron metabolism proteins inactive, thus encouraging iron pooling (Rawat *et al*., 2021). The mitochondrial iron accumulated by DOX catalyzes the production of ROS as described above. This type of cell death is also strictly related to lipid peroxidation and is responsible for part of the cardiac damage produced by DOX (Christidi and Brunham, 2021).

Pyroptosis or immunogenic cell death is an inflammation-promoting type of cell death induced by DOX binding to gasdermin D and E that further activates caspases and cell death (Vitale *et al*., 2024). Simultaneously, this effect can trigger T-cell immune responses which can attack tumor cells. Although undesired for the implication in CTOX, this consequence of DOX could be used to enhance the efficiency of immunotherapies when administered in the same treatment regimen (Gabizon *et al*., 2025).

Cell death initiated by calcium homeostasis dysregulation is produced by doxorubicinol, which similarly to ferroptosis, is able to increase the intracellular Ca^{2+} levels by inhibiting the sodium-calcium exchanger protein. In muscle cells, calcium overload activates calpains which activates caspases and increase ROS production, thus leading to cell death (Rawat *et al*., 2021).

Cardiotoxicity. In the case of DOX administration, CTOX is the most daunting side effect, especially in childhood cancer survivors. Pediatric patients can often tolerate more aggressive treatment regimens, most likely due to fewer comorbidities, better organ function and different drug metabolism than adults. Yet, this population is more affected by tardive side effects of cancer treatments that can alter their quality of life, and physicians should be more aware of warning signs of side effects than in adults (Helms *et al*., 2023; van den Boogaard *et al*., 2022).

Medical practitioners became aware of the cardiac damage produced by anthracyclines shortly after daunorubicin was introduced in clinical use. In the two "Letters to the Editor" of The Lancet journal in 1969, authors described their cases and outcomes, and advised their colleagues on methods to prevent CTOX, mainly by reserving daunorubicin use only for young patients affected by leukemia and avoiding combined therapies with drugs that increase the cardiotoxic effects (Bonadonna and Monfardini, 1969).

Symptoms of CTOX are often "silent" at the onset of the disease or can go unnoticed because they are non-specific. This is the case for intermittent chest pain, fatigue, shortness of breath, vertigo, heart palpitations or limb swelling because in the absence of cardiovascular diagnostic tests, these can be easily attributed to other conditions (Rawat *et al*., 2021).

A challenging fact to acknowledge is that gender bias heavily impacts CVD diagnosis. This is proven by the fact that mortality rate is higher in women compared to men (Townsend *et al*., 2022). Although several factors such as smoking, obesity, menopause and pregnancy are contributors to risk increase, these should not affect the diagnostic process (Sliwa *et al*., 2021). An increasing pool of evidence shows that CVD symptoms are often disregarded or misinterpreted by medical practitioners as anxiety, depression, or just fatigue in general. These misconceptions, along with the tendency to understate the severity of their symptoms lead to less women receiving referrals to a cardiologist (Al Hamid *et al*., 2024; Berg Gundersen *et al*., 2017; Ezekowitz *et al*., 2020; Sliwa *et al*., 2021).

Despite extensive research, the mechanism of CTOX development is still unclear, especially in the case of late-onset or chronic CTOX, occurring years after treatment completion. For acute forms of the disease, tissue uptake of DOX increases oxidative stress, thus promoting cell damage and apoptotic pathways.

In the case of CTOX occurring long after treatment, the only evidence-supported hypothesis is that DOX treatment promotes an aging phenotype in heart tissue, which cannot be identified by current diagnosis methods (Linders *et al*., 2024).

As described in Chapter II, a method for preventing or curing CTOX is not yet available. The most clinically effective solution seems to stand in a combination of both conventional and traditional medicine, along with a non-invasive

screening of patients to identify subclinical CTOX swiftly and implement treatment as soon as possible.

Materials and Methods

The study adhered to the requirements of the European Directive 2010/63/EU and national legislation 43/2014 regarding the protection of animals used for scientific purposes. The protocol was approved by the Committee on the Ethics of Animal Experiments of Babeş-Bolyai University (14.172/02.11.2021) and was compliant to the ARRIVE guidelines. Adult male Wistar rats (of average weight 250 g at the beginning of the experiment) were housed in the Animal Laboratory Facility (Zoobase) at the Babeş-Bolyai University in Cluj-Napoca. Throughout the experiment, animals received free access to standard diet and water, were gently handled and were kept in standard cages on a 12-hour light-dark cycle.

The treatment protocol has been described previously (Anca *et al*., 2024). Briefly, a cumulative dose of 15 mg/kg DOX hydrochloride was divided into 4 weekly doses and administered intravenously via tail vein. Control group was treated with vehicle, in the same manner. Tissues were harvested post-treatment and at 4 weeks post-treatment for the acute and chronic manifestations of toxicity, respectively.

For ultrastructural analysis, the protocol described by Crăciun & Barbu-Tudoran (2013). Briefly, collected heart and liver tissues were quicky fixed in 2.7% glutaraldehyde, washed and post-fixed in 2% osmium tetraoxide. After acetone dehydration, samples were embedded in Epon 812 resin (Electron Microscopy Science USA). Section trimmings were performed using a Leica UC6 microtome, and then sections were placed on electron microscope grids. After double contrasted using uranyl acetate (UranyLess, Electron Microscopy Science, USA), grids were examined using a Jeol JSM 1010 (Japan) transmission electron microscope. Images were post-edited for contrast using Adobe Photoshop software. Transmission electron microscopy images were obtained at the "Constantin Crăciun" Electron Microscopy Center.

For histopathological analysis, heart, aorta, liver and kidney sections were prepared for hematoxylin-eosin (H&E) staining. Briefly, tissue fragments were isolated and fixed in a 5% neutral formalin solution, for approximately 72 hours. After paraffin embedding, multiple sections were cut at 5 µm thickness and mounted onto glass slides. After dewaxing in xylene and rehydration, sections were stained using the standard H&E procedure. Slides were then investigated using an Optika 510 LD1 microscope with a 5MP charge-coupled device (CCD) camera.

Results

Ultrastructural analysis of heart tissue from Control rats shows normal cell architecture at both time-points, with clearly delineated myofibrils running parallel to each other. Sarcomeres are visibly separated by Z membranes. Mitochondria are electron dense and contain unaltered cristae. The euchromatic nucleus contains a well-defined nucleolus (Fig. 1A-D).

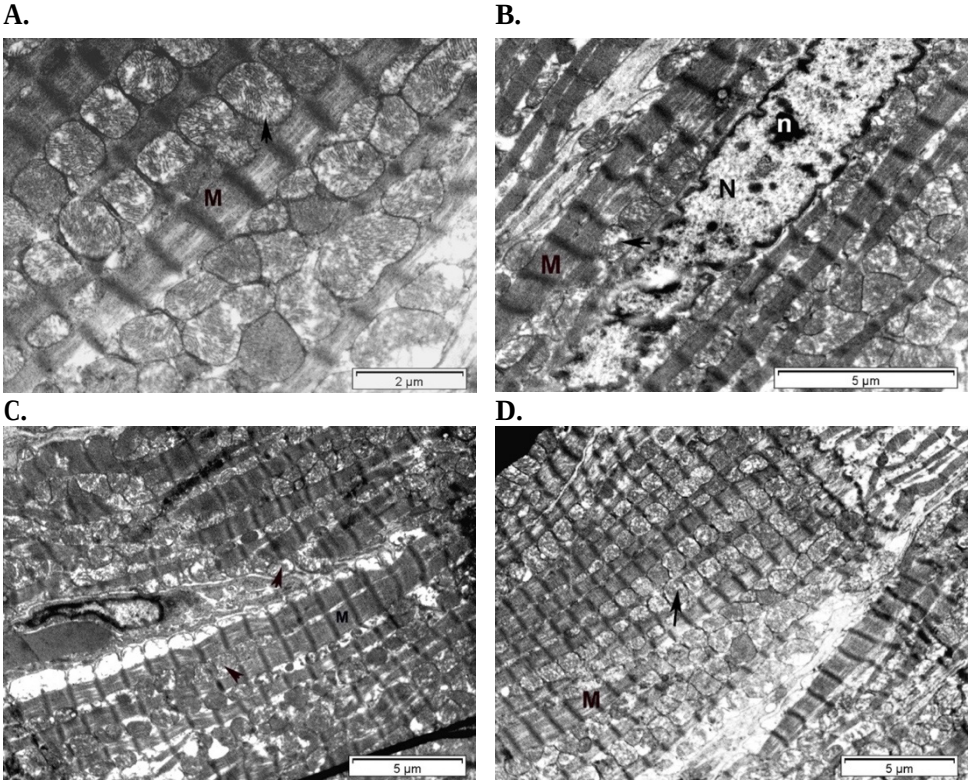

Figure 1. Electron micrographs of Control group myocardial tissue, post-treatment (A, B) and 4 weeks post-treatment (C, D). A. Well-defined myofibrils (M), running parallel to each other, with visible sarcomeres delimited between two neighboring Z membranes; B. between myofibrils, rows of mitochondria are observed (marked by arrows); these mitochondria are normally electron dense, with intact cristae. The nucleus (N) is euchromatic, with well-differentiated nucleolus (n); C. normal cardiomyocytes, with normally arranged myofibrils (M) in parallel rows; D. normal arrangement of mitochondria (marked by arrows), parallel to myofibrils.

DOX group ultrastructural analysis showed extensive damage at both time-points, with disorganized myofibrils, collapsed mitochondrial cristae and numerous lipid and collagen deposits (Fig. 2A-B). Post-treatment, nuclei were predominantly

heterochromatic, with irregular shapes and surrounded by vacuolization processes. Interestingly, at this time-point we mainly observed damaged mitochondria, which appear to fuse at 4 weeks post-treatment (Fig. 2C-D).

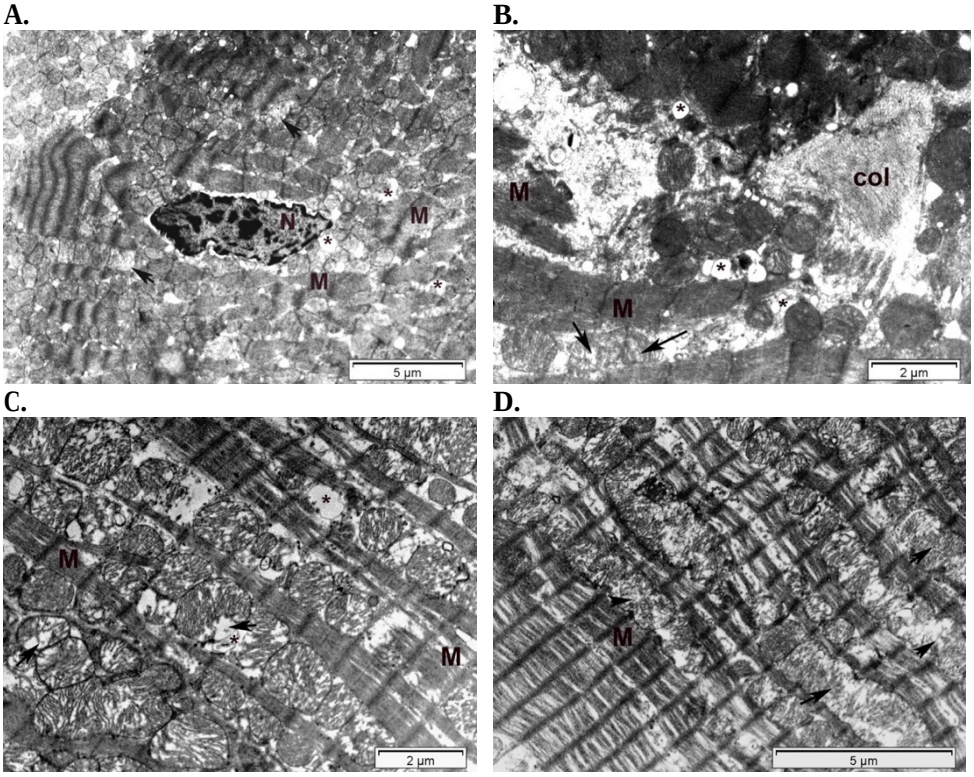

Figure 2. Electron micrographs of DOX group myocardial tissue, post-treatment (A, B) and 4 weeks post-treatment (C, D). A. disorganized myofibrils (M), mitochondria (marked by arrows) with collapsed cristae, heterochromatic nucleus (N) of irregular shape and perinuclear cytoplasmic vacuolisation; B. intracellular lipid droplets (marked by *) and collagen deposits; C. degraded myofibrils (M), with denatured content; disorganized mitochondrial cristae (arrow); lipid droplets in between mitochondria (marked by *); D. some mitochondria show fusion-like behavior, as a response to intense metabolic stress.

All histological samples were collected only after the completion of the 4-week course of treatment. Histological analysis of heart sections from the Control group show intact tissue structure (Fig. 3A-B). In DOX group, disorganized muscle bundles along with leukocyte infiltrates and visible microhemorrhages (MHs) are seen (Fig. 3C-D). Additionally, post-treatment cardiomyocytes show excentric nuclei position and rarefied cytoplasm (Fig. 3E).

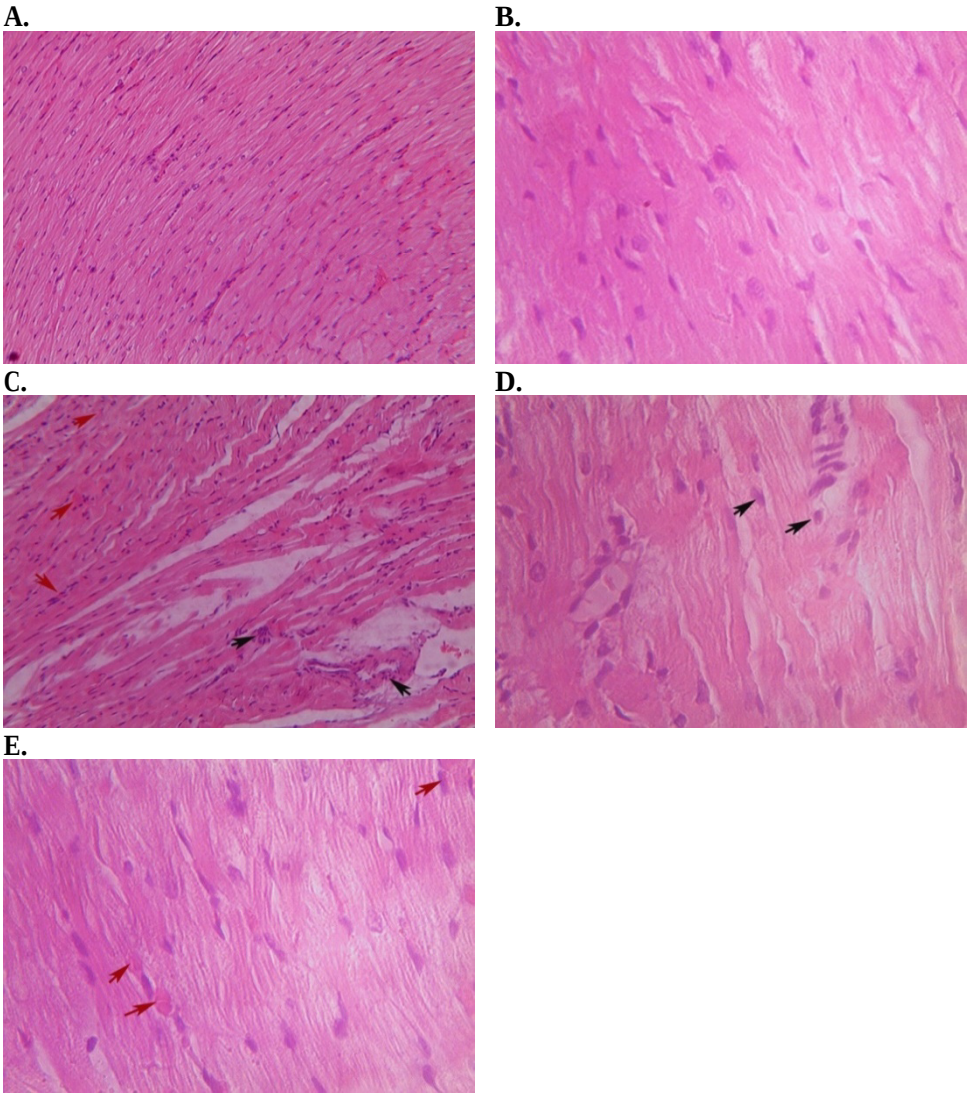

Figure 3. Heart sections of Control and DOX groups, H&E staining. A and B. Control post treatment. Both images are showing normal tissue architecture x10 for A, x40 for B; C. DOX, post-treatment, x10; D and E. DOX, post-treatment, x40. Black arrows indicate leukocyte infiltrates and red arrows indicate MH.

Control group aorta samples show normal cell and tissue structure. In tunica media, rows of smooth muscle cells are intercalated with parallel elastic fibers (Fig. 4A). DOX treatment caused a relative thinning of the tunica media and thickening of the tunica adventitia (Fig. 4B).

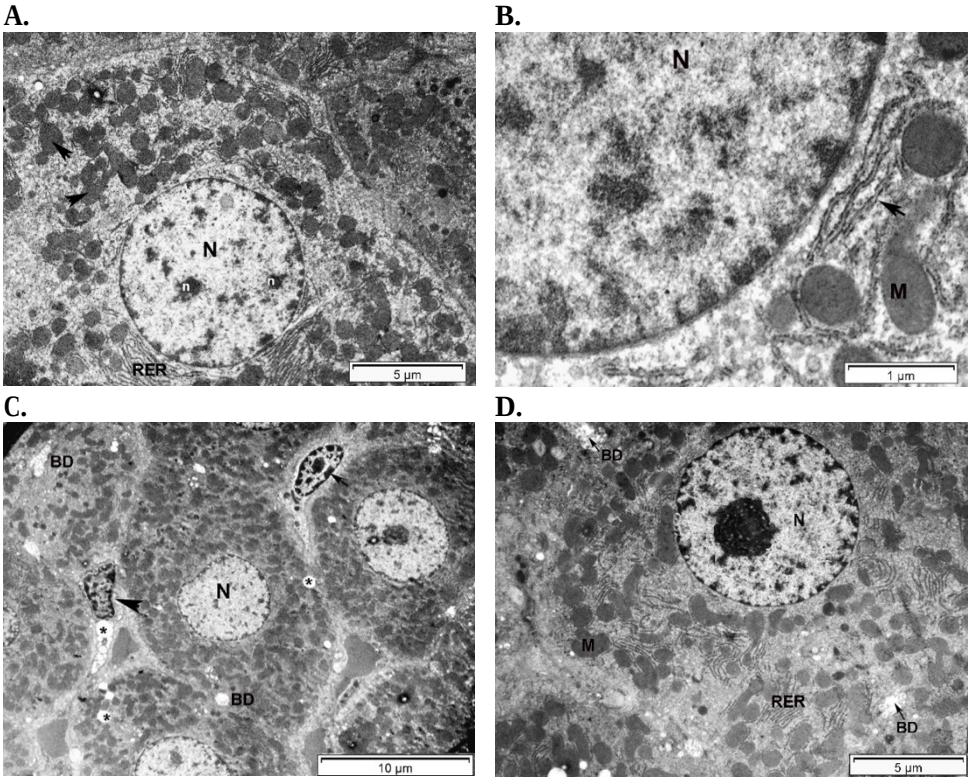

Figure 4. Electron micrographs of Control group liver tissue, post-treatment (A, B) and 4 weeks post-treatment (C, D). A. hepatocyte with euchromatic, spherical nucleus (N) and 2 nucleoli (n), and parallel RER. Mitochondria (arrows) are normal electron dense; **B.** mitochondrial complexes surrounded by RER (arrow); **C.** parenchymal cells with central, well-defined nucleus (N), hepatocyte microvilli present in the BD and in the Disse spaces, lipid droplets (marked by *) in hepatocytes and Ito cells (thick arrow), and a Kupffer cell (thin arrow); **D.** hepatocyte with euchromatic nucleus and large nucleolus, RER and mitochondrial complexes, and BD. RER – rough endoplasmic reticulum; BD –bile duct.

Control group TEM images for both time-points show normal cellular architecture. Post-treatment, hepatocytes have euchromatic, spherical nuclei surrounded by numerous cisternae of the rough endoplasmic reticulum (RER) and mitochondria (Fig. 4A-B). Additionally, at 4 weeks post-treatment, few lipid droplets can be observed in hepatic stellate cells and hepatocytes (Fig. 4B-C). At both time-points, DOX led to SER and RER proliferation (Fig. 5AD), and hepatocyte apoptosis (Fig. 5B-C), with more cellular damage observed at 4-week post-treatment (Fig. 5E).

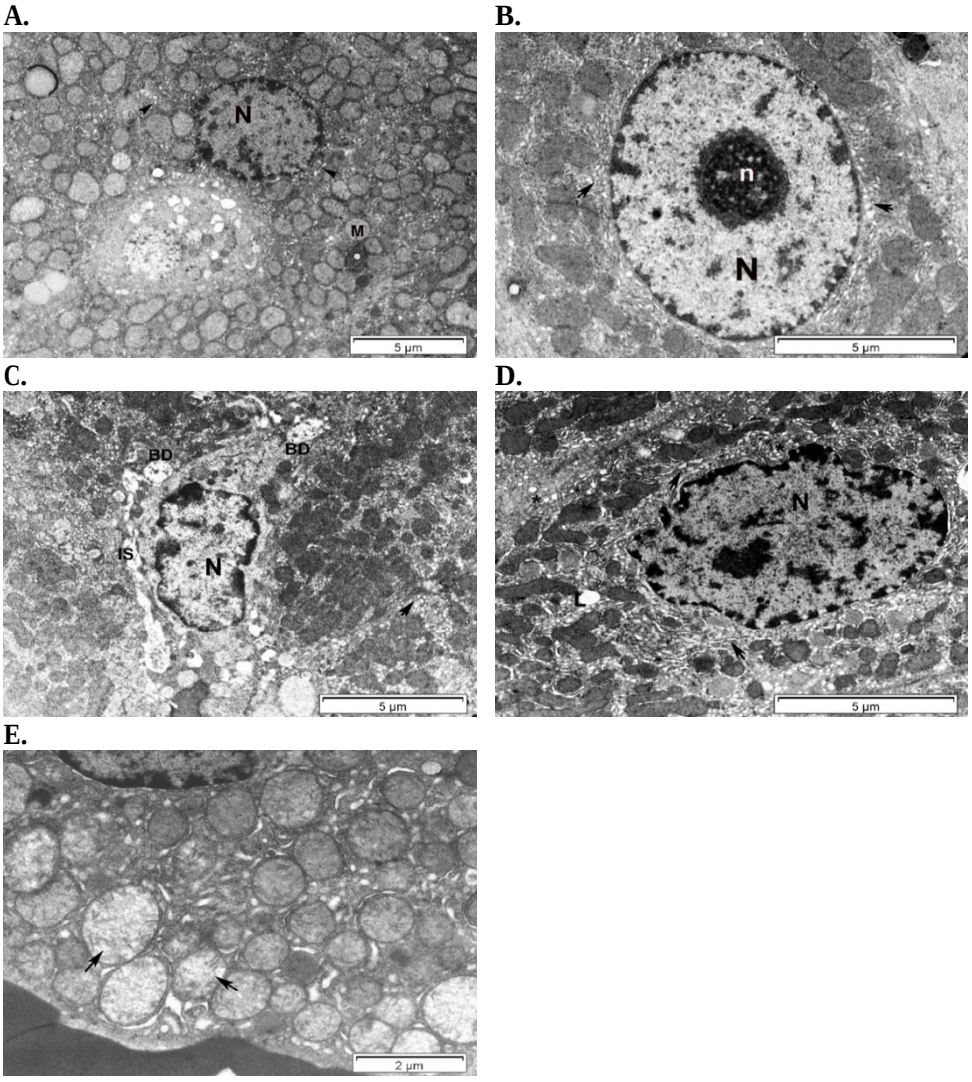

Figure 5. Electron micrographs of DOX group liver tissue, post-treatment (A, B) and 4 weeks post-treatment (C, D, E). A. dilated membrane vesicles of SER (arrows); cellular debris as remnants of a probably apoptotic cell; **B.** cell with intact nucleus (N) and nucleolus (n); massive proliferation of endoplasmic reticulum; **C.** hepatocyte with irregular nuclear (N) shape and enlarged intercellular space (IS), and bile ducts with altered hepatocyte microvilli (BD), proliferation of SER (arrow); **D.** hepatocyte with heterochromatic irregular nucleus (N), proliferation of SER and RER (arrow and *, respectively); **E.** faulty mitochondria, with damaged cristae (arrows) between dilated RER profiles. SER – smooth endoplasmic reticulum; RER – rough endoplasmic reticulum.

To further evaluate the extent of structural disruption caused by DOX, histological sections were examined. Micrographs of livers from the Control group show physiological tissue structure, with normal hepatocytes, arranged in continuous plates around the centrilobular vein (CV) (Fig. 6A-B). DOX treatment led to loss of normal tissue architecture, with enlargement of the CV and dilated sinusoids, along with inclusions between hepatocytes (Fig. 6C). At week 4 post-treatment, we observed the proliferation of biliary ducts, along with enlarged Disse spaces and disorganized cytoplasm in hepatocytes (Fig. 6D-E).

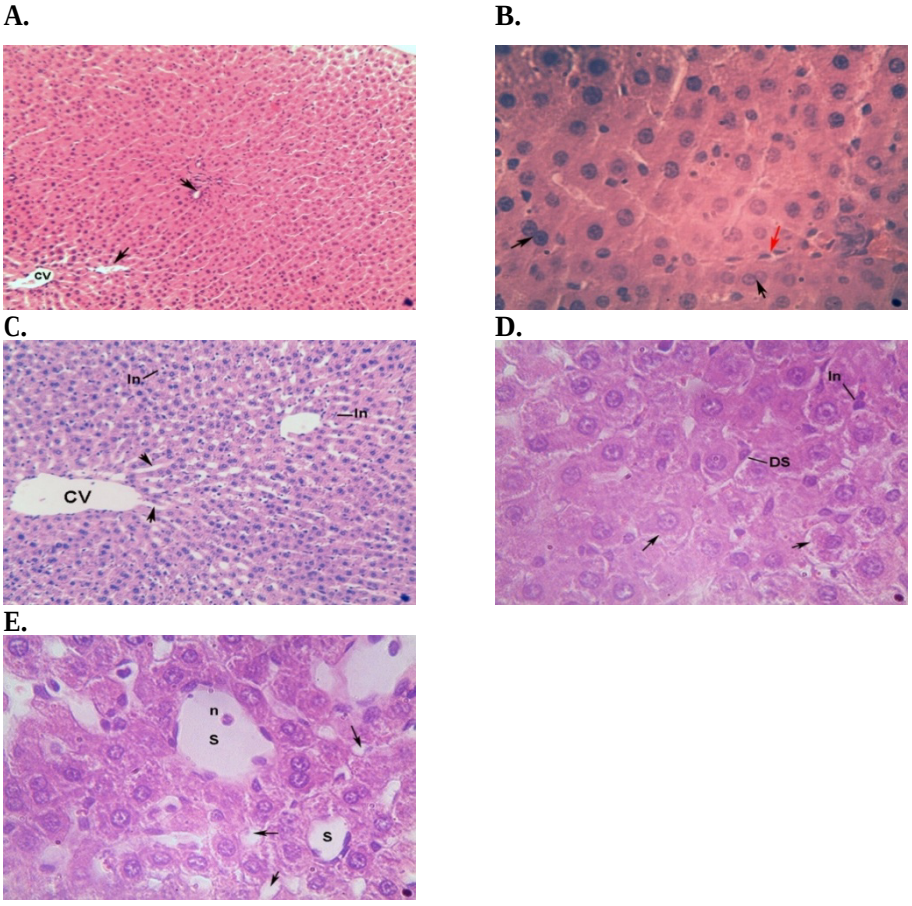

Figure 6. Liver sections of Control and DOX groups, H&E staining. A and B. Control post-treatment images, showing intact tissue structure. Centrilobular vein (CV), sinusoid capillaries (black arrows in A), Kupffer cell (red arrow in B), binucleated cells (black arrows in B); x10 for A, x40 for B; C. DOX, post-treatment image with CV, sinusoid dilatation (arrows) and inclusion bodies (In), x10; D. DOX post-treatment, indicating disorganized cytoplasm marked by arrows, enlarged Disse spaces (DS) and cell inclusions (In), x40; E. DOX post-treatment, S indicates liver sinusoids, proliferated biliary ducts (arrows), a neutrophil in a sinusoid capillary (n), x40.

Kidney photomicrographs for the Control group show normal tissue architecture, with round, well-conturated glomeruli (G) and visible macula densa (MD). Proximal (PT) and distal convoluted tubes (DT) are normal appearing (Fig. 7A-B). DOX group, similar to the other organs analyzed, shows irreversible structural damage. Vascular injury is reflected by multiple MH spots visible at both magnifications used. Some nuclei have pyknotic appearance and are displaced beyond the cellular boundary, which indicates active apoptotic or necrotic processes. The majority of renal corpuscles were severly deformed (Fig. 7C-E).

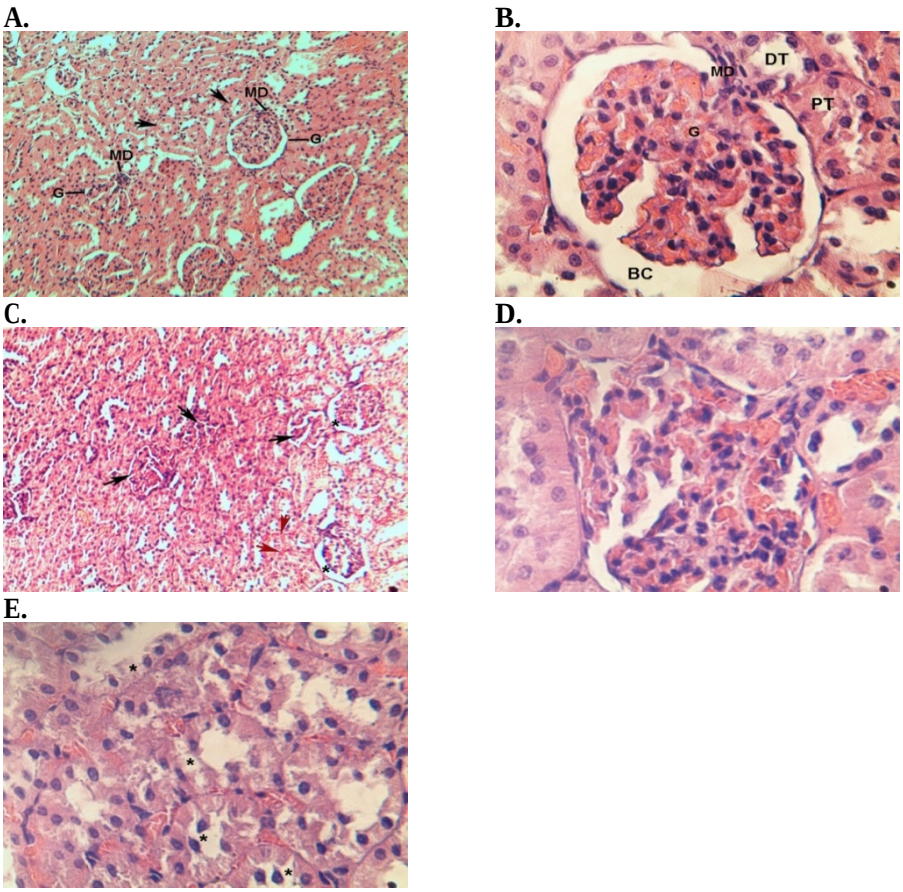

Figure 7. Kidney sections of Control and DOX groups, H&E staining. A. In Control group post-treatment, arrows indicate normal tubular epithelium (arrows) and glomeruli (G); at some glomeruli, the macula densa (MD) can also be seen; x10; B. A round renal corpuscle in the Control group with normal Bowman capsule (BC) and capillary loops of the glomerule (G); the macula densa (MD) is visible at the beginning of distal tube (DT), near a loop of the proximal tube (PT); x40; C. DOX group, post-treatment. The renal corpuscles (G, black arrows) are deeply altered, with missing, or enlarged Bowman

capsule (*); the red arrows indicate MH foci; x10; D. A renal corpuscle in the DOX-treated group. The Bowman capsule is not visible and the capillary loops of the glomerule are disorganized; x40. E. DOX group, post-treatment. Renal tubes with altered cells, some of them with disrupted membrane and nuclei beyond the cell boundaries (*); x40.

Discussion

Cardiomyocytes are mitochondria-rich cells, due to their intense need for energy. Under improper conditions such as extreme oxidative stress, mitochondria undergo inner and outer membrane fusion. As a result, the fused mitochondria share their contents to maintain normal function (Adebayo *et al*., 2021). This quick process is mediated by mitofusins (MFN1 and MFN2) for the outer membrane, whereas the inner mitochondrial membrane is fused by optic atrophy 1 (OPA1). Errors in this process are lethal, as proven by mutant mice experiments (Pernas and Scorrano, 2016).

As DOX is an inhibitor of mitochondrial fusion and fission (Ding *et al*., 2022), this process was not observed at the end of treatment (Fig. 2AB). However, as shown in Fig. 4B, we observed fused mitochondria at 4 weeks post-treatment. This suggests that after DOX exposure ends, although cardiomyocytes show clear signs of severe energy impairment, partially impaired mitochondria are adapting to the altered cell environment and compensating for the damage.

Collagen accumulation in cardiac muscle has been observed in DOX treated mice (He *et al*., 2020b) and is a sign of hypertrophy and fibrosis (Levick *et al*., 2019). One of the ways DOX could intensify collagen production and deposition is by upregulation of Adamts19, which we observed in our transcriptomic analysis of heart tissue after the same DOX protocol (results not published).

Morphological evaluation of heart sections revealed oxidative-stress related tissue injury, which presents with separation of myofibers, inflammatory cell infiltration and microhemorrhages (MH) (Fig. 3 D-E).

The effects DOX exhibits on the liver need as much attention as the heart, because the oxidative stress produced by DOX metabolism greatly impacts the liver (Gedikli *et al*., 2023). DOX heavily impacts the liver by decreasing lipid metabolism which ultimately leads to nonalcoholic steatohepatitis (Timm *et al*., 2022). DOX-induced liver injury is led by ROS overproduction, which lowers the activity of the antioxidant molecules (glutathione peroxidase, superoxide dismutase, catalase and glutathione) (Prasanna *et al*., 2020).

In our previous study, we demonstrated that DOX produces hyperlipidemia which continues to worsen even after treatment completion (Anca *et al*., 2024). Given that liver dysfunction is a widely recognized risk factor for cardiovascular disease (Lee *et al*., 2020), these results consolidate the importance of early protective strategies for patients undergoing chemotherapy regimens that include DOX.

Hepatocyte ballooning, which is characterized by enlarged cells with dilated cytoplasm, is a sign of injury and metabolism alteration as a response to DOX-induced oxidative stress (Bonnet *et al*., 2022; Fatani *et al*., 2022). This was observed in post-treatment liver sections (Fig. 7 D-E), which may also predict a prolonged alteration of the tissue following DOX exposure. Additionally, we observed numerous MH spots caused by sinusoidal endothelial barrier integrity disruption (Fig. 7C-E). This type of endothelial injury could be attributed to DOX-induced mitochondrial dysfunction: excessive ROS production in the mitochondria can trigger a ROS-induced ROS release mechanism, which in turn damages the endothelial wall (He *et al*., 2020a).

The smooth ER is an important player in lipid metabolism, especially in the liver. ER proliferation is a known stress marker associated with cardiovascular and metabolic diseases (Sozen and Ozer, 2017) by increasing fatty acid synthesis (Zhou *et al*., 2022).

Histological analysis of kidney tissue revealed severe and progressive renal damage. As indicated by multiple MH spots, vascular injury seems to be an ongoing process (Fig. 8C). Additionally, the altered appearance of the renal corpuscles adjacent to the MH and displacement of the nuclei beyond the cellular membrane collectively highlight the degree of DOX toxicity in the kidney (Fig. 8BC). As in the other tissues, DOX-kidney injury is likely caused by oxidative stress and inflammation (Hussain *et al*., 2021; Szalay *et al*., 2015).

Conclusion

The present work provides additional information regarding histological and ultrastructural effects of DOX on tissues to build upon previous research on the evaluation of circulating biomarkers. The systemic impact of DOX is manifested through oxidative stress, vascular injury and lipid dysregulation.

In all organs analyzed, DOX led to progressive tissue dysfunction manifested as apoptotic-like cell appearance, myofibrillar disarray and vascular damage and immune cell infiltration. These results, combined with our previous observations, emphasize the need of a multifaceted therapeutic approach to DOX toxicity centered on reduction of oxidative stress to non-target organs.

References

Adebayo, M., Singh, S., Singh, A.P. & Dasgupta, S. (2021). Mitochondrial fusion and fission: the fine-tune balance for cellular homeostasis. *FASEB J. 35(6)*, 321620. https://doi.org/10.1096/fj.202100067R

Al Hamid, A., Beckett, R., Wilson, M., Jalal, Z., Cheema, E., Al-Jumeily OBE, D., Coombs, T., Ralebitso-Senior, K. & Assi, S. (2024). Gender bias in diagnosis, prevention, and treatment of cardiovascular diseases: a systematic review. *Cureus 16(2)*, e54264. https://doi.org/10.7759/cureus.54264

Anca, E., Sabău, F., Vădan, A., Marinescu, M., Licărete, E., Roşioru, C., Stoica, A.D., Dobre, C. & Banciu, M. (2024). Assessment of circulating biomarkers in a rat model of doxorubicin-induced cardiotoxicity. *Stud. Univ. Babes Bolyai Biol. 69(2)*, 7–22. https://doi.org/10.24193/subbbiol.2024.2.01

Berg Gundersen, A.E., Sørlie, T. & Bergvik, S. (2017). Women with coronary heart disease – making sense of their symptoms and their experiences from interacting with their general practitioners. *Health Psychol. Behav. Med. 5*, 29–40. https://doi.org/10.1080/21642850.2016.1263574

Bonadonna, G. Monfardini, S. (1969). Cardiac toxicity of daunorubicin. *Lancet 293(7599)*, 837-838. https://doi.org/10.1016/s0140-6736(69)92093-5

Bonnet, L., Alexandersson, I., Baboota, R.K., Kroon, T., Oscarsson, J., Smith, U. & Boucher, J. (2022). Cellular senescence in hepatocytes contributes to metabolic disturbances in NASH. *Front. Endocrinol. (Lausanne) 13*, 957616. https://doi.org/10.3389/fendo.2022.957616

Cassinelli, G. (2016). The roots of modern oncology: from discovery of new antitumor anthracyclines to their clinical use. *Tumori 2016(3)*, 226-235. https://doi.org/10.5301/tj.5000507

Christidi, E. & Brunham, L.R. (2021). Regulated cell death pathways in doxorubicin-induced cardiotoxicity. *Cell Death. Dis. 12(4)*, 339. https://doi.org/10.1038/s41419-021-03614-x

Craciun, C. & Barbu-Tudoran, L. (2013). Identification of new structural elements within "porosomes" of the exocrine pancreas: a detailed study using high-resolution electron microscopy. *Micron 44*, 137-142. https://doi.org/10.1016/j.micron.2012.05.011

Ding, M., Shi, R., Cheng, S., Li, M., De, D., Liu, C., Gu, X., Li, J., Zhang, S., Jia, M., Fan, R., Pei, J. & Fu, F. (2022). Mfn2-mediated mitochondrial fusion alleviates doxorubicin-induced cardiotoxicity with enhancing its anticancer activity through metabolic switch. *Redox Biol. 52*, 102311. https://doi.org/10.1016/j.redox.2022.102311

Ezekowitz, J.A., Savu, A., Welsh, R.C., McAlister, F.A., Goodman, S.G. & Kaul, P., (2020). Is there a sex gap in surviving an acute coronary syndrome or subsequent development of heart failure? *Circulation 142(23)*, 2231-2239. https://doi.org/10.1161/CIRCULATIONAHA.120.048015

Fatani, A., Baothman, O., Shash, L., Abuaraki, H., Zeyadi, M., Hosawi, S., Altayb, H. & Abo-Golayel, M. (2022). Hepatoprotective effect of date palm fruit extract against doxorubicin intoxication in Wistar rats: in vivo and in silico studies. *Asian Pac. J. Trop. Biomed. 12(8)*, 357-366. https://doi.org/10.4103/2221-1691.350184

Forman, H.J., Maiorino, M. & Ursini, F. (2010). Signaling functions of reactive oxygen species. *Biochemistry. 49(5)*, 835-842. https://doi.org/10.1021/bi9020378

Gabizon, A.A., Gabizon-Peretz, S., Modaresahmadi, S. & La-Beck, N.M. (2025). Thirty years from FDA approval of pegylated liposomal doxorubicin (Doxil/Caelyx): an updated analysis and future perspective. *BMJ Oncol. 4(1)*, e000573. https://doi.org/10.1136/bmjonc-2024-000573

Gedikli, E., Barış, V.Ö., Yersal, N., Dinçsoy, A.B., Müftüoğlu, S.F. & Erdem, A. (2023). Taurine protects doxorubicin-Induced hepatotoxicity via its membrane-stabilizing effect in rats. *Life 13(10)*, 2031. https://doi.org/10.3390/life13102031

He, H., Wang, L., Qiao, Y., Zhou, Q., Li, H., Chen, S., Yin, D., Huang, Q. & He, M., (2020a). Doxorubicin induces endotheliotoxicity and mitochondrial dysfunction via ROS/eNOS/NO pathway. *Front. Pharmacol. 10*, 1531. https://doi.org/10.3389/fphar.2019.01531

He, Q., Wang, F., Ryan, T.D., Chalasani, M. & Redington, A.N. (2020b). Repeated remote ischemic conditioning reduces doxorubicin-induced cardiotoxicity. JACC *CardioOncol. 2(1)*, 41-52. https://doi.org/10.1016/j.jaccao.2020.01.005

Helms, L., Guimera, A.E., Janeway, K.A. & Bailey, K.M. (2023). Innovations in cancer treatment of children. *Pediatrics 152(6)*, e2020301539. https://doi.org/10.1542/peds.2023-061539

Hussain, M.A., Abogresha, N.M., Abdelkader, G., Hassan, R., Abdelaziz, E.Z. & Greish, S.M. (2021). Antioxidant and anti-inflammatory effects of crocin ameliorate doxorubicin-induced nephrotoxicity in rats. *Oxid. Med. Cell Longev. 2021*, 8841726. https://doi.org/10.1155/2021/8841726

Jones, I.C. & Dass, C.R. (2022). Doxorubicin-induced cardiotoxicity: causative factors and possible interventions. *J. Phar. Pharmacol. 74(12)*, 167-1688. https://doi.org/10.1093/jpp/rgac063

Kciuk, M., Gielecińska, A., Mujwar, S., Kołat, D., Kałuzińska-Kołat, Ż., Celik, I. & Kontek, R. (2023). Doxorubicin—an agent with multiple mechanisms of anticancer activity. *Cells 12(4)*, 659. https://doi.org/10.3390/cells12040659

Lee, J., Choi, M.K. & Song, I.S., (2023). Recent advances in doxorubicin formulation to enhance pharmacokinetics and tumor targeting. *Pharmaceuticals 16(6)*, 802. https://doi.org/10.3390/ph16060802

Lee, S.F., Luque-Fernandez, M.A., Chen, Y.H., Catalano, P.J., Chiang, C.L., Wan, E.Y.F., Wong, I.C.K., Chen, M.H. & Ng, A.K. (2020). Doxorubicin and subsequent risk of cardiovascular diseases among survivors of diffuse large B-cell lymphoma in Hong Kong *Blood Adv. 4(20)*, 5107-5117. https://doi.org/10.1182/BLOODADVANCES.2020002737

Leung, A.W.Y., Amador, C., Wang, L.C., Mody, U. V. & Bally, M.B. (2019). What drives innovation: the canadian touch on liposomal therapeutics. *Pharmaceutics 11(3)*, 124 https://doi.org/10.3390/pharmaceutics11030124

Levick, S.P., Soto-Pantoja, D.R., Bi, J., Hundley, W.G., Widiapradja, A., Manteufel, E.J., Bradshaw, T.W. & Meléndez, G.C. (2019). Doxorubicin-induced myocardial fibrosis involves the neurokinin-1 receptor and direct effects on cardiac fibroblasts. *Heart Lung Circ. 28(10)*, 1598-1605 https://doi.org/10.1016/j.hlc.2018.08.003

Li, X.R., Cheng, X.H., Zhang, G.N., Wang, X.X. & Huang, J.M. (2022). Cardiac safety analysis of first-line chemotherapy drug pegylated liposomal doxorubicin in ovarian cancer. *J. Ovarian Res. 15(1)*, 96. https://doi.org/10.1186/s13048-022-01029-6

Linders, A.N., Dias, I.B., López Fernández, T., Tocchetti, C.G., Bomer, N. & Van der Meer, P. (2024). A review of the pathophysiological mechanisms of doxorubicin-induced cardiotoxicity and aging. *npj Aging 10(1)*, 9. https://doi.org/10.1038/s41514-024-00135-7

Liu, Y., Chen, S., Wen, Z., Meng, J., Yang, Y., Zhang, Y., Wang, J. & Cao, X. (2024). Comparative pharmacokinetics of free doxorubicin and a liposomal formulation in cats following intravenous administration. *Front. Vet. Sci. 11*, 1353775. https://doi.org/10.3389/fvets.2024.1353775

Mattioli, R., Ilari, A., Colotti, B., Mosca, L., Fazi, F. & Colotti, G. (2023). Doxorubicin and other anthracyclines in cancers: activity, chemoresistance and its overcoming. *Mol Aspects Med. 93,* 101205. https://doi.org/10.1016/j.mam.2023.101205

Pernas, L. & Scorrano, L. (2016). Mito-morphosis: mitochondrial fusion, fission, and cristae remodeling as key mediators of cellular function. *Annu Rev Physiol. 78* 505-531. https://doi.org/10.1146/annurev-physiol-021115-105011

Prasanna, P.L., Renu, K. & Valsala Gopalakrishnan, A. (2020). New molecular and biochemical insights of doxorubicin-induced hepatotoxicity. *Life Sci. 250*, 117599. https://doi.org/10.1016/j.lfs.2020.117599

Rawat, P.S., Jaiswal, A., Khurana, A., Bhatti, J.S. & Navik, U. (2021). Doxorubicin-induced cardiotoxicity: An update on the molecular mechanism and novel therapeutic strategies for effective management. *Biomed. Pharmacother. 2021*, 111708. https://doi.org/10.1016/j.biopha.2021.111708

Shandilya, M., Sharma, S., Das, P.P. & Charak, S. (2020). Molecular-level understanding of the anticancer action mechanism of anthracyclines, in: Arnouk, H., Hassan, B.A.R. (Eds.), Advances in precision medicine oncology. *IntechOpen*, *9*. https://doi.org/10.5772/intechopen.94180

Shi, S., Chen, Y., Luo, Z., Nie, G. & Dai, Y. (2023). Role of oxidative stress and inflammation-related signaling pathways in doxorubicin-induced cardiomyopathy. *Cell Commun. Signal. 21(1)*, 61. https://doi.org/10.1186/s12964-023-01077-5

Sliwa, K., van der Meer, P., Petrie, M.C., Frogoudaki, A., Johnson, M.R., Hilfiker-Kleiner, D., Hamdan, R., Jackson, A.M., Ibrahim, B., Mbakwem, A., Tschöpe, C., Regitz-Zagrosek, V., Omerovic, E., Roos-Hesselink, J., Gatzoulis, M., Tutarel, O., Price, S., Heymans, S., Coats, A.J.S., Müller, C., Chioncel, O., Thum, T., de Boer, R.A., Jankowska, E., Ponikowski, P., Lyon, A.R., Rosano, G., Seferovic, P.M. & Bauersachs, J. (2021). Risk stratification and management of women with cardiomyopathy/heart failure planning pregnancy or presenting during/after pregnancy: a position statement from the Heart Failure Association of the European Society of Cardiology Study Group on peripartum cardiomyopathy. *Eur. J. Heart Fail. 23(4)*, 527-540. https://doi.org/10.1002/ejhf.2133

Sozen, E. & Ozer, N.K. (2017). Impact of high cholesterol and endoplasmic reticulum stress on metabolic diseases: an updated mini-review. *Redox Biol. 12*, 456-461. https://doi.org/10.1016/j.redox.2017.02.025

Szalay, C.I., Erdélyi, K., Kökény, G., Lajtár, E., Godó, M., Révész, C., Kaucsár, T., Kiss, N., Sárközy, M., Csont, T., Krenács, T., Szénási, G., Pacher, P. & Hamar, P. (2015). Oxidative/nitrative stress and inflammation drive progression of doxorubicin-induced renal fibrosis in rats as revealed by comparing a normal and a fibrosis-resistant rat strain. *PLoS One 10(6)*, e0127090. https://doi.org/10.1371/journal.pone.0127090

Timm, K.N., Ball, V., Miller, J.J., Savic, D., West, J.A., Griffin, J.L. & Tyler, D.J. (2022). Metabolic Effects of doxorubicin on the rat liver assessed with hyperpolarized MRI and metabolomics. *Front. Physiol. 12*, 782745. https://doi.org/10.3389/fphys.2021.782745

Townsend, N., Kazakiewicz, D., Lucy Wright, F., Timmis, A., Huculeci, R., Torbica, A., Gale, C.P., Achenbach, S., Weidinger, F. & Vardas, P. (2022). Epidemiology of cardiovascular disease in Europe. *Nat. Rev. Cardiol. 19(2)*, 133-143. https://doi.org/10.1038/s41569-021-00607-3

van den Boogaard, W.M.C., Komninos, D.S.J. & Vermeij, W.P. (2022). Chemotherapy side-effects: not all DNA damage is equal. *Cancers (Basel). 14(3)*, 627. https://doi.org/10.3390/cancers14030627

van der Zanden, S.Y., Qiao, X. & Neefjes, J. (2021). New insights into the activities and toxicities of the old anticancer drug doxorubicin. *FEBS J. 288(21)*, 6095-6111. https://doi.org/10.1111/febs.15583

Vitale, R., Marzocco, S. & Popolo, A. (2024). Role of oxidative stress and inflammation in doxorubicin-induced cardiotoxicity: a brief account. *Int. J. Mol. Sci. 25(13)*, 7477. https://doi.org/10.3390/ijms25137477

WHO (World Health Organization) (2023). World Health Organization model list of essential medicines – 23rd list, 2023, in: The selection and use of essential medicines 2023. web annex A. https://www.who.int/publications/i/item/WHO-MHP-HPS-EML-2023.02

Xie, S., Sun, Y., Zhao, X., Xiao, Y., Zhou, F., Lin, L., Wang, W., Lin, B., Wang, Z., Fang, Z., Wang, L. & Zhang, Y. (2024). An update of the molecular mechanisms underlying anthracycline induced cardiotoxicity. *Front. Pharmacol. 15, 1406247*. https://doi.org/10.3389/fphar.2024.1406247

Yang, F., Teves, S.S., Kemp, C.J. & Henikoff, S. (2014). Doxorubicin, DNA torsion, and chromatin dynamics. *Biochim Biophys. Acta. Rev. Cancer 1845(1)*, 84-89. https://doi.org/10.1016/j.bbcan.2013.12.002

Zhou, L., Shen, H., Li, X. & Wang, H. (2022). Endoplasmic reticulum stress in innate immune cells - a significant contribution to non-alcoholic fatty liver disease. *Front. Immunol. 13*, 951406. https://doi.org/10.3389/fimmu.2022.951406